

Supplementary Information

Effects of heating rate and deposition cycle on the structural, optical, and photoelectrocatalytic properties of electrodeposited hematite films

Pannan I. Kyesmen^{1,2*}, William Pooe¹, Nolwazi Nombona³, Mmantsae Diale^{1*}

¹Physics Department, University of Pretoria, Private Bag X20, Hatfield 0028, South Africa.

²Physics Department, Joseph Sarwuan Tarka University Makurdi (previously, Federal University of Agriculture Makurdi) P.M.B. 2373, Makurdi, Benue State, Nigeria.

³Chemistry Department, University of Pretoria, Private Bag X20, Hatfield 0028, South Africa.

Corresponding author's e-mail addresses: pannan.kyesmen@tuks.co.za; mmantsae.diale@up.ac.za.

Table S1. The FWHM, crystal size, microstrain, and dislocation density of electrodeposited hematite thin films.

Sample	Bragg angle (2 θ)	FWHM (degrees)	Crystal size (nm)	Strain ϵ x 10 ⁻³	Dislocation density ρ x 10 ¹⁵ Lin/m ²
2°C/min	35.766	0.424	19.7	5.78	2.58
10°C/min	35.787	0.288	29.0	3.92	1.19
35°C/min	35.792	0.284	29.4	3.86	1.16
Rapid annealing	35.776	0.324	25.8	4.41	1.50
ED-15C	36.153	0.368	22.7	4.98	1.94
ED-30C	35.843	0.319	26.2	4.32	1.46
ED-60C	35.787	0.288	29.0	3.90	1.19
ED-80C	35.741	0.278	30.0	3.76	1.11

Table S2. A comparison of the experimental 2-theta values for the XRD peaks obtained for the samples and the standard reference values given in the JCPDS file number 00-033-0664.

XRD planes (hkl)	Experimental 2 theta value (degrees)	Reference standard 2 theta value: JCPDS no. 00-033-0664 (degrees)
12	24.28	24.14
104	33.31	33.15
110	35.81	35.61
113	40.98	40.86
24	49.62	49.48
116	54.18	54.09
214	62.54	62.45
300	64.14	63.99

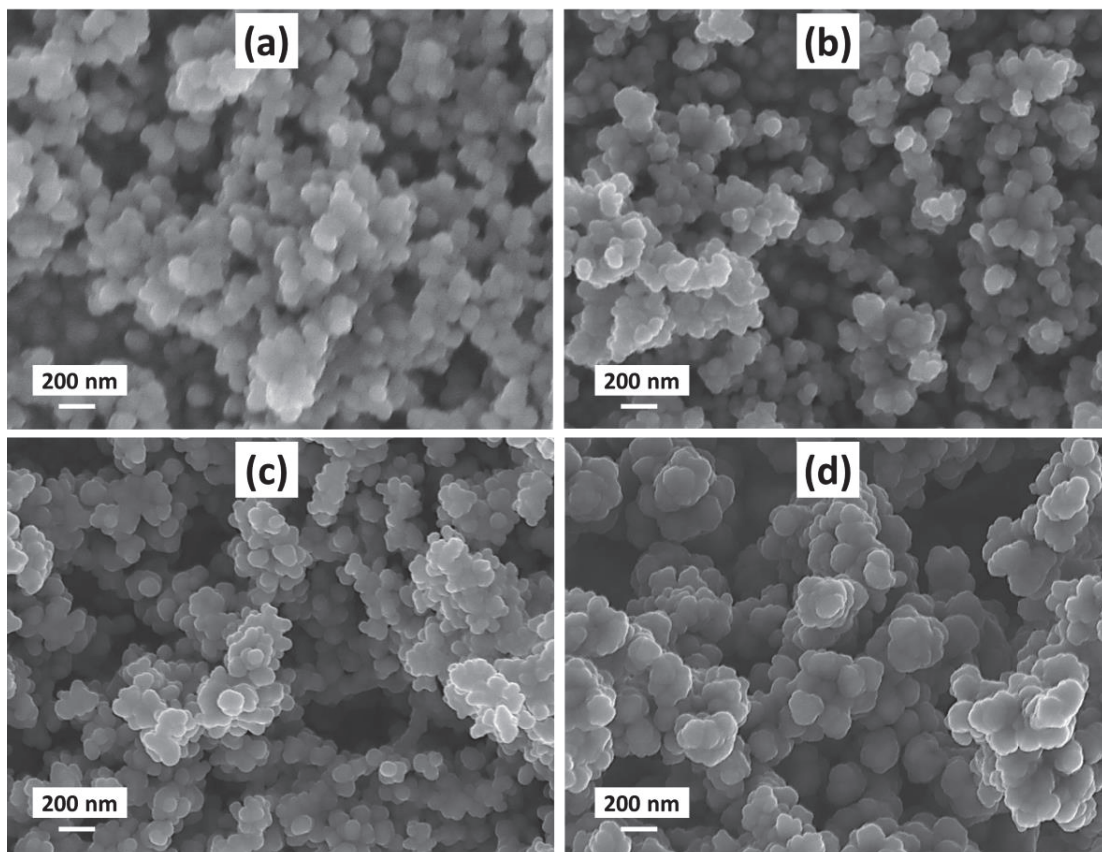


Fig. S1. SEM images of (a) ED-15C, (b) ED-30C, (c) ED-60C, and (d) ED-80C hematite samples

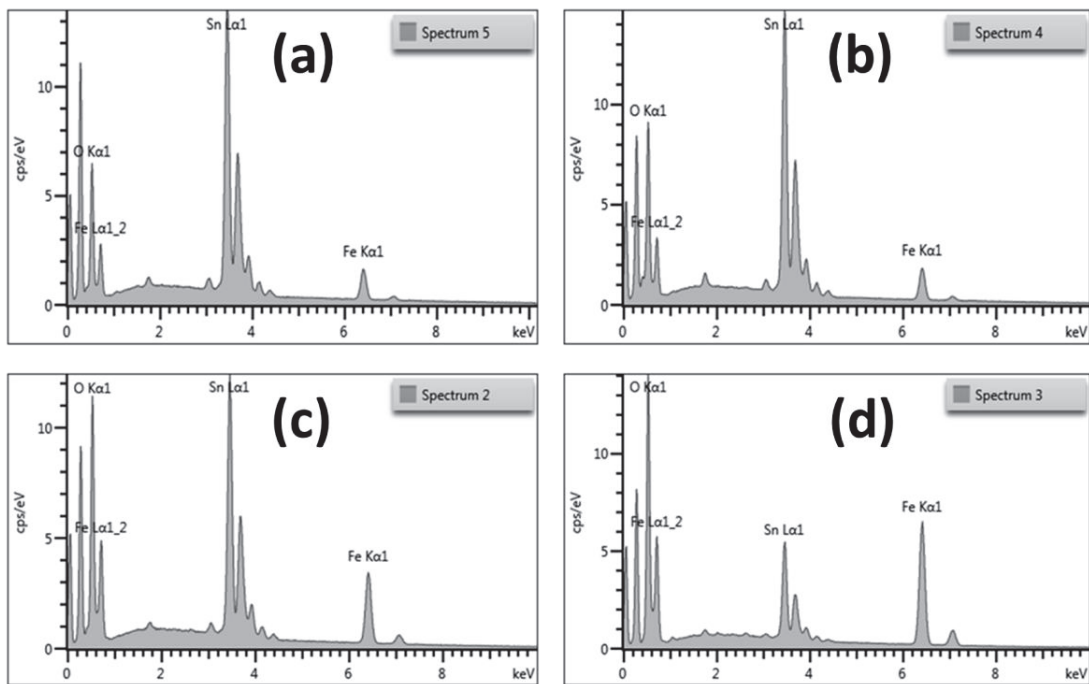


Fig. S2. EDS results for hematite films deposited at (A) 15, (B) 30, (C) 60, and (D) 80 deposition cycle numbers respectively.

Mott-Schottky relation

The Mott-Schottky (M-S) engaged in evaluating the donor densities and flat band potentials of the electrodeposited hematite films from the M-S plots given in Fig. 6 is given in Equation S1.

$$\frac{1}{C^2} = \frac{2}{\epsilon_0 \epsilon e A^2 N_D} \left(V - V_{fb} - \frac{KT}{e} \right) \quad (S1)$$

where C denotes the interfacial capacitance, A represents the surface area of the photoelectrode, $\epsilon = 80$ and represents the dielectric constant of hematite, ϵ_0 denotes the permittivity of free space, e is the electronic charge, V is the applied potential, K is the Boltzmann constant and T represents the temperature [1]. The value of A , used for each of the electrodes was about 1.8 cm^2 : the surface area of the photoanodes dipped into the electrolyte.

The first linear regions of the M-S plots in Fig. 6 of the main manuscript were fitted and the slope (S) of the plots was used to calculate the N_D values for the samples in line with the relation in equation S2 deduced from Equation S1.

$$S = \frac{2}{\epsilon_0 \epsilon e A^2 N_D} \quad (S2)$$

The S values obtained for the plots were positive slope obtained as expected, which confirms the n-type semiconducting property of hematite [2]. The linear region of the M-S plots of the samples was extrapolated to intercept the potential V_0 along the V -axis where $\frac{1}{C^2} = 0$. This simplifies equation S1 to $V_0 = V_{fb} + (KT/e)$ where the V_{fb} values can be extracted. Table 1 of the main manuscript presents approximate values of N_D and V_{fb} calculated for electrodeposited hematite photoanodes.

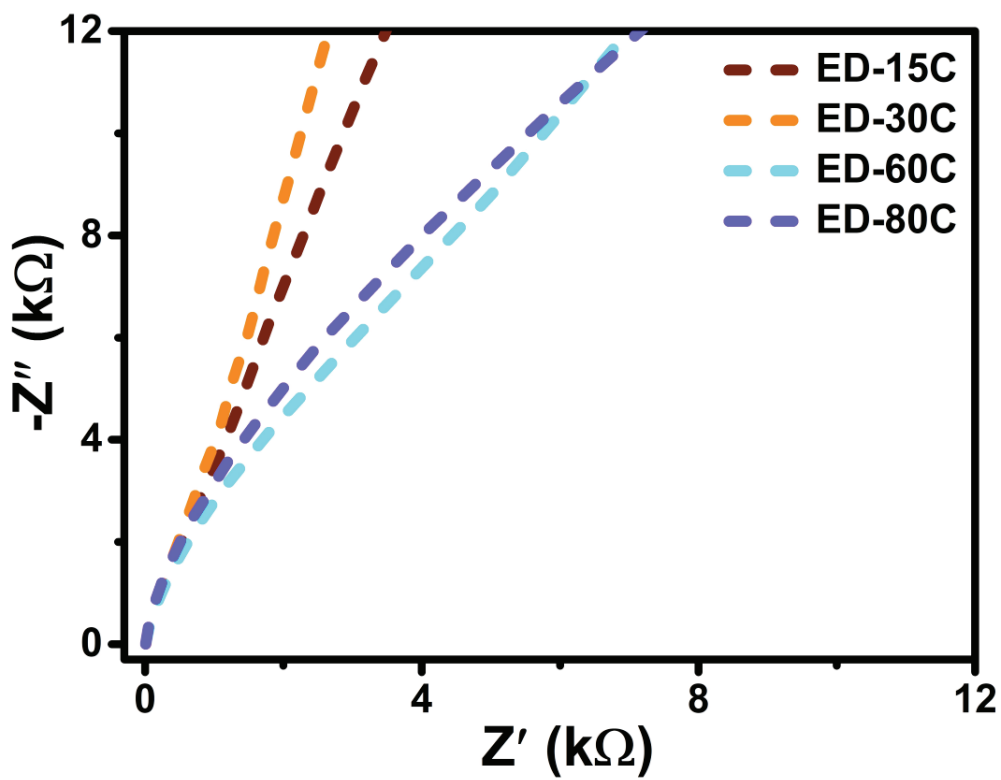


Fig. S3. Expanded view of the PEIS Nyquist plots for electrodeposited hematite photoanodes prepared at different deposition cycles.

Reference

1. Liang, Y., C.S. Enache, and R. van de Krol, *Photoelectrochemical Characterization of Sprayed [alpha]-Fe₂O₃ Thin Films: Influence of Si Doping and SnO₂ Interfacial Layer*. International Journal of Photoenergy, 2008. **2008**.
2. Iandolo, B., et al., *Correlating flat band and onset potentials for solar water splitting on model hematite photoanodes*. RSC advances, 2015. **5**(75): p. 61021-61030.